Electronic Supplementary Material (ESI) for New Journal of Chemistry

Supporting Informantion

Nickel molybdenum oxide nanoarray as efficient and stable electrocatalyst for overall water splitting

Xiaoshuang Zhang,[a] Hui Su,[b] and Xiaoqiang Du [c*]

a. School of Science, North University of China, Taiyuan 030051, People's Republic of China.

b. School of environment and safety, North University of China, Taiyuan 030051, People's Republic of China.

c. School of Chemical Engineering and Technology, North University of China, Taiyuan 030051, People's Republic of China. E-mail: duxq16@nuc.edu.cn

Materials

$Ni(NO_3)_2$, $Na_2MoO_4 \cdot 2H_2O$, NH_4F and KOH are obtained from Sigma-Aldrich and used directly not further purified. Nickel foam (NF) was purchased from Shenzhen Green and Creative Environmental Science and Technology Co. Ltd.

Preparation of a-$NiMoO_4$ nanosheet arrays on nickel foam

First, the Ni foam (2×5 cm^2) was immersed in 3.0M HCl to remove the surface oxide layer of substrate before drying in an oven. The a-$NiMoO_4$ nanosheet arrays were obtained by a simple hydrothermal process. 1.5 mmol $Ni(NO_3)_2 \cdot 6H_2O$, 1.5 mmol $Na_2MoO_4 \cdot 2H_2O$ and 5 mmol NH_4F were dissolved in a mixture of 25 mL ethyl alcohol and 25 mL H_2O under vigorous magnetic stirring for 10 min. The substrate was transferred to a Teflon-lined stainless-steel autoclave. Next, the autoclave was sealed and maintained at 160 °C for 4 h. Then, the precursor was removed and cleaned by ultrasonication for 5 min to remove the loosely attached products on the surface. Afterwards, $NiMoO_4$ nanosheet was obtained by annealing at 400 °C in a N_2 atmosphere for 2 h at a heating rate of 10 °C min^{-1}.

Characterization of materials

The phase composition and purity of the materials are identified using X-ray powder diffraction (XRD) by Xpert-Pro MPD diffractometer with Cu Kα radiation. The morphology of the materials is researched using scanning electron microscopy (SEM) images with Tescan MAIA3 XMH, and the chemical elements of the materials are cataloged using X-ray photoelectron spectra (XPS) tests on PerkinElmer PHI 5000C. The corresponding TEM elemental mapping images were measured using transmission electron microscopy (TEM) with JEOL 2010.

Faraday efficiency measurement

The same volume of gas sample in the headspace of the electrolytic cell was withdrawn by a SGE gas-tight syringe and analyzed by gas chromatography (GC). The H_2 in the sampled gas was separated by passing through a 2 m × 3 mm packed molecular sieve 5A column with an Ar carrier gas and quantified by a Thermal Conductivity Detector (TCD)(Shimadzu GC-9A).

DFT computation details

The DFT calculations were performed using the Cambridge Sequential Total Energy Package (CASTEP) with the plane-wave pseudo-potential method. The geometrical structures of the (001) plane of $NiMoO_4$ were optimized by the generalized gradient approximation (GGA) methods. The Revised Perdew-Burke-Ernzerh of (RPBE) functional was used to treat the electron exchange correlation interactions. A Monkhorst Pack grid k-points of 3×3×2 and a plane-wave basis set cut-off energy of 400 eV were used for integration of the Brillouin zone. The structures were optimized for energy and force convergence set at 0.03 eV/A and 1.0×10^{-5} eV, respectively. A self-consistence field of 2.0×10^{-6} eV/atom was applied. A vacuum space as large as 15.0 A was used to avoid periodic interactions.

Table S1. Comparison of water splitting performance for b-$NiMoO_4$/NF with other non–noble–metal water splitting catalysts under alkaline conditions.

Catalyst	**Cell voltage**	**Res.**
b-$NiMoO_4$	**1.55V**	**This work**
a-$NiMoO_4$	**1.65V**	**This work**
Co_9S_8@NOSC-900	1.60V	[1]
Ni-Fe-MOF	1.55V	[2]
Al-CoP	1.56V	[3]
$Co_3(PO_4)_2$	1.48V	[4]
$Ni(OH)_2$@Ni_3S_2	1.57V	[5]
Mo/Mn-Ni_xS_y	1.49V	[6]
Ni_3S_2	1.73V	[7]

Table S2. The atomic percent of b-$NiMoO_4$

element	weight percentage	atomic percent
O K	39.24	74.77
Ni K	29.35	15.24
Mo K	31.41	9.98
Total	100.00	

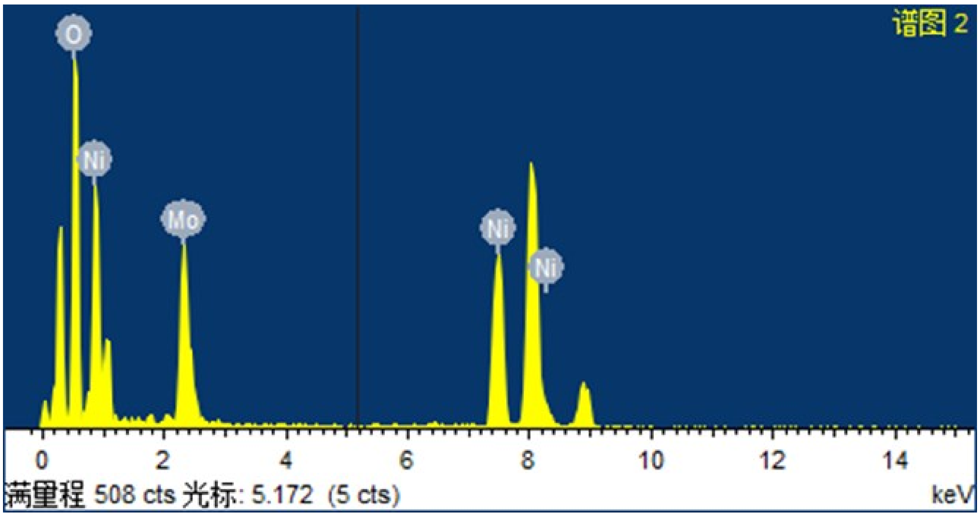

Fig. S1EDS spectroscopy of the b-$NiMoO_4$.

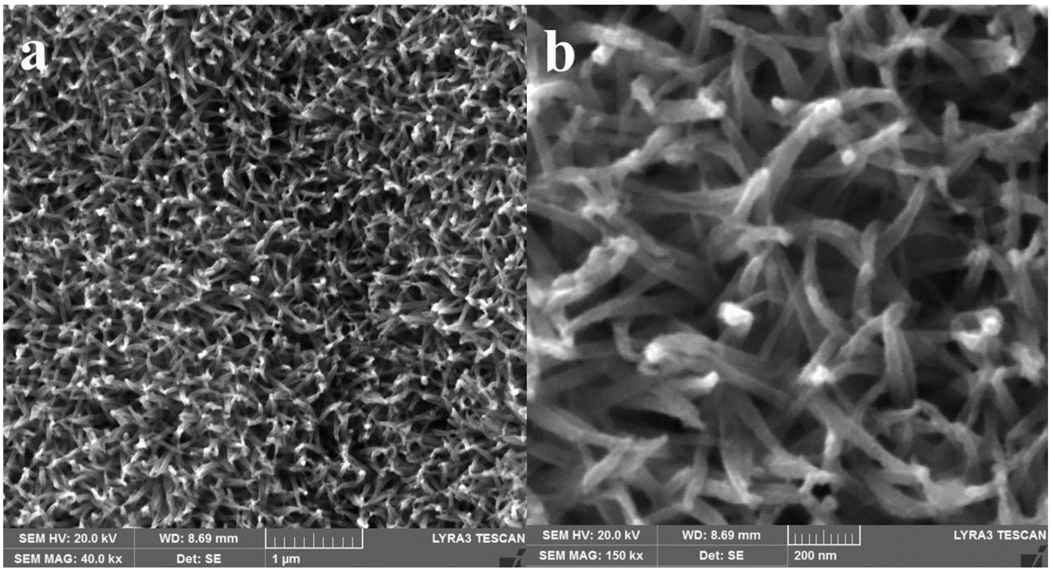

Fig. S2 The SEM of the $NiMoO_4$ synthesized without the addition of NH_4F.

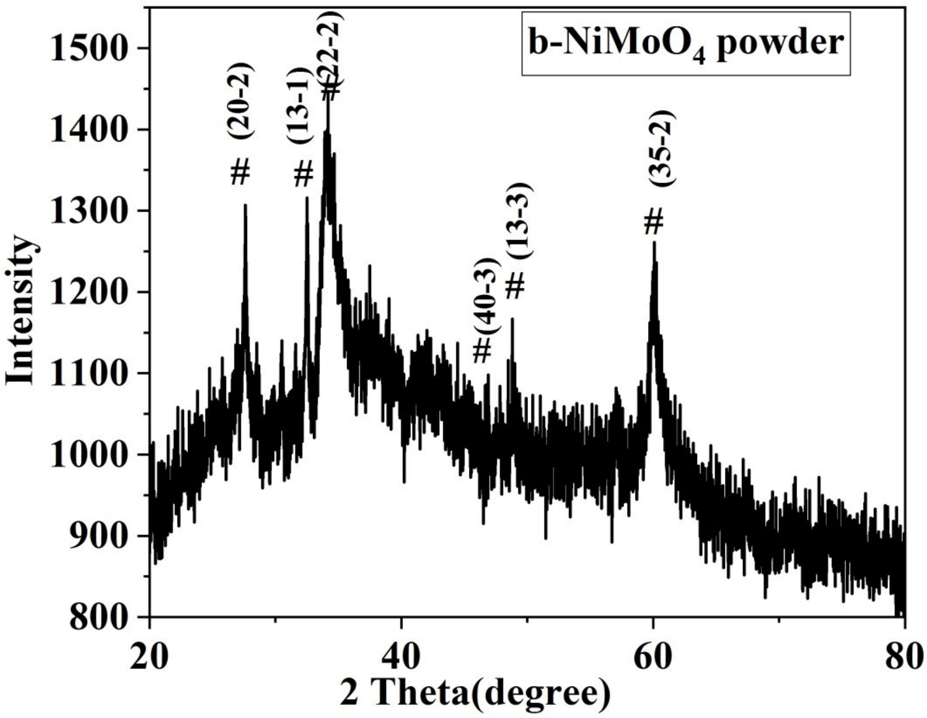

Fig. S3 XRD of the b-$NiMoO_4$ powder.

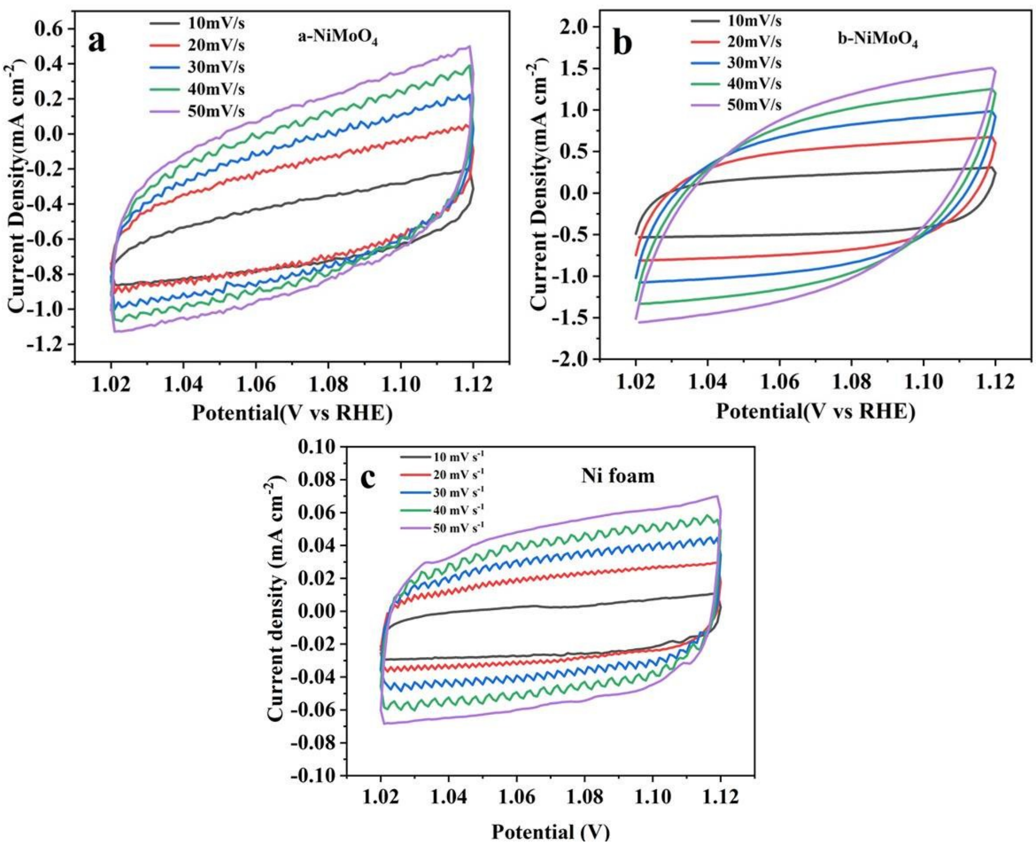

Fig. S4 CV_S of a-$NiMoO_4$ (a), b-$NiMoO_4$ (b) and Ni foam (c)with different scan rates (10-50 mV s^{-1}) in the region of 1.02-1.12V *vs* RHE.

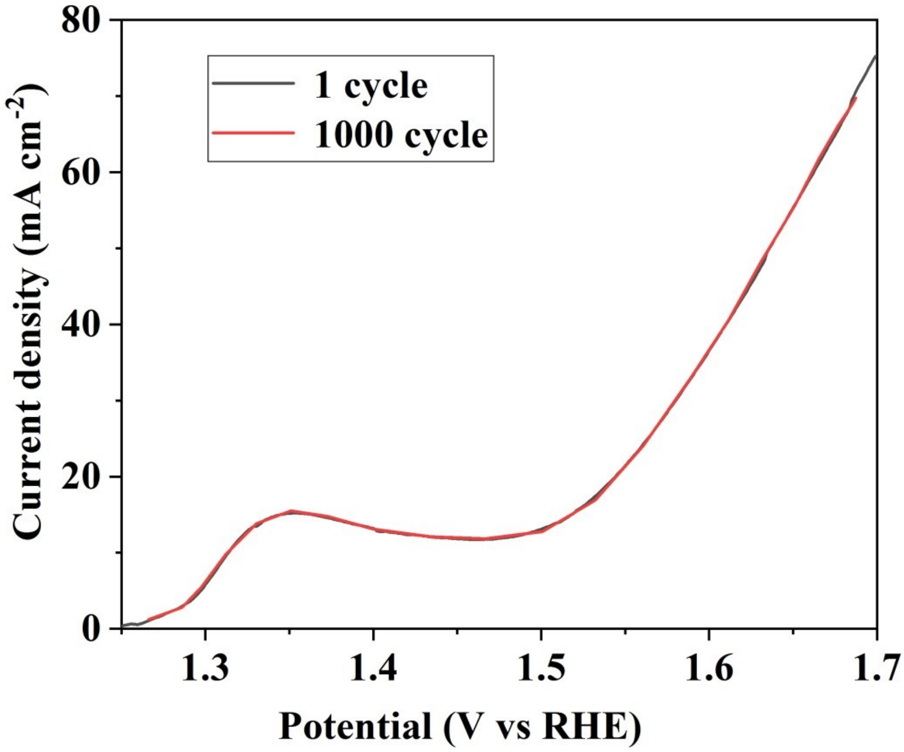

Fig. S5 OER polarization curves for the b-$NiMoO_4$ before and after 1000 cycles of the accelerated stability test.

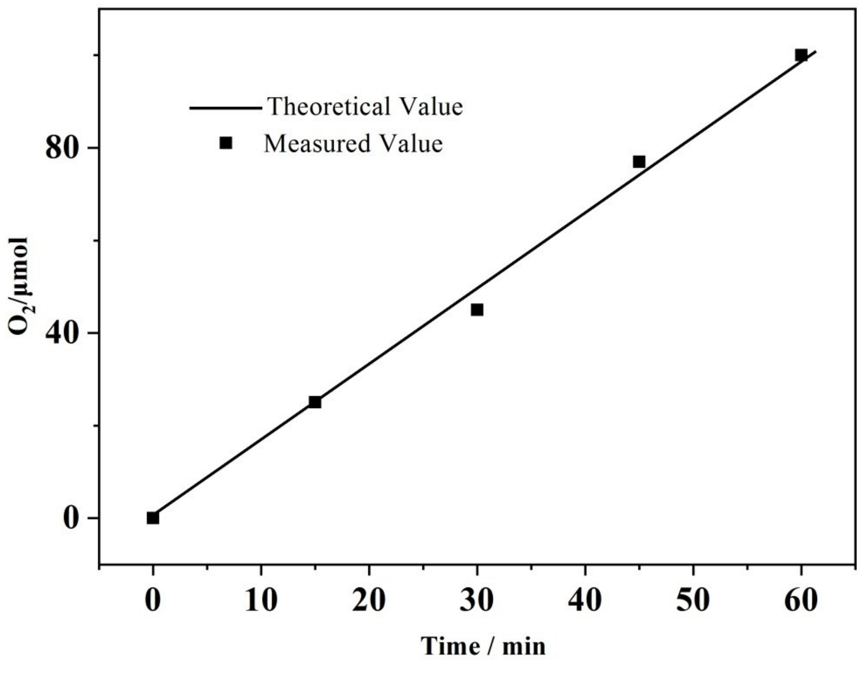

Fig. S6 Electrocatalytic efficiency of O_2 production over b-$NiMoO_4$ at a potential of ca. 1.53 V, measured for 60 min.

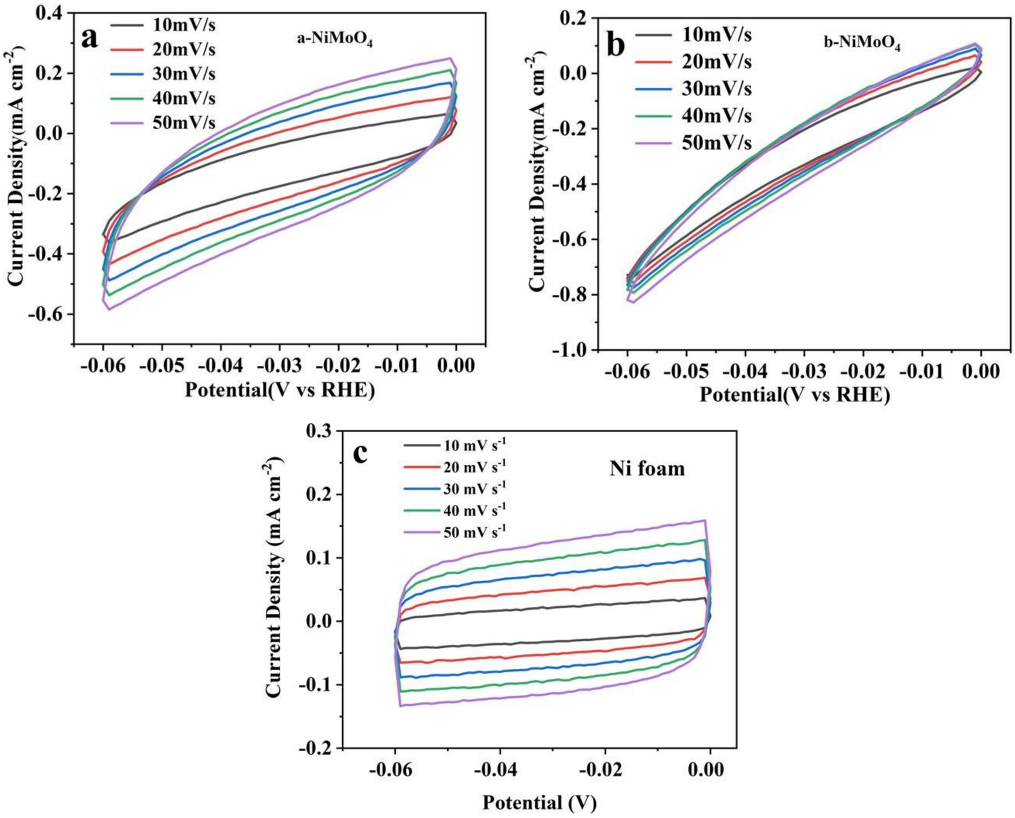

Fig. S7 CV_S of a-$NiMoO_4$ (a), b-$NiMoO_4$ (b) and Ni foam (c) with different scan rates (10-50 mV s^{-1}) in the region of -0.06-0.00V *vs* RHE.

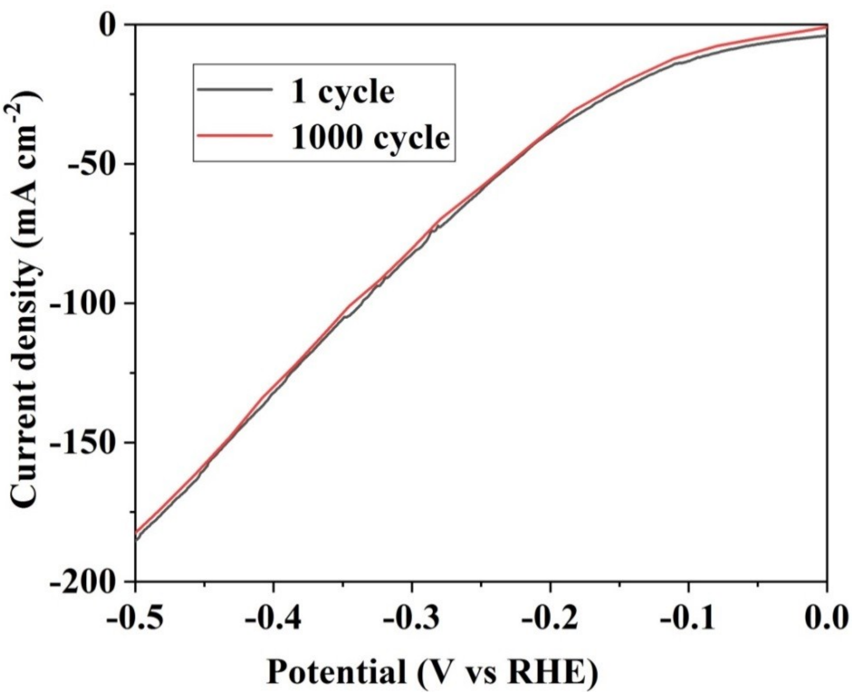

Fig. S8 HER polarization curves for the b-$NiMoO_4$ before and after 1000 cycles of the accelerated stability test.

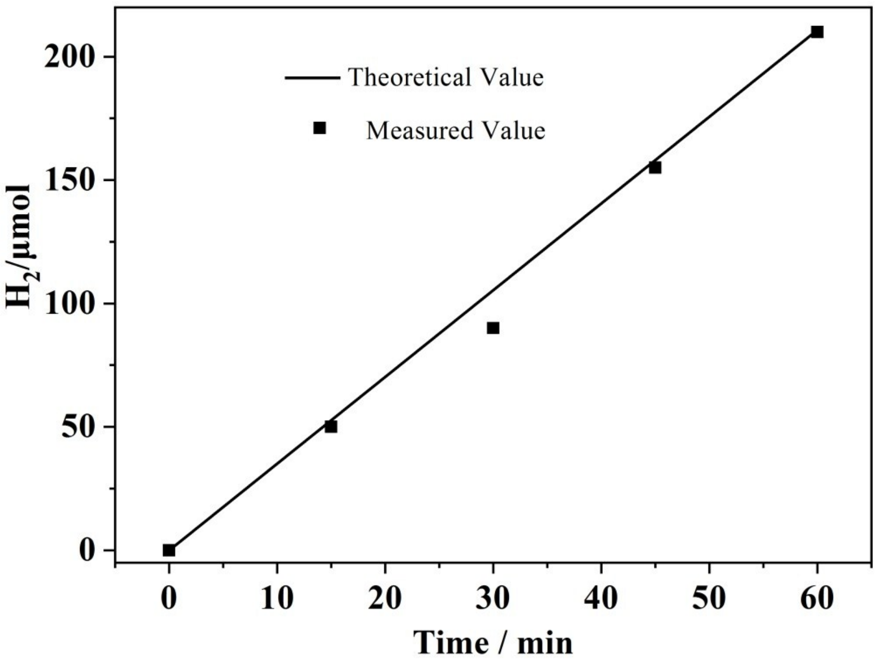

Fig. S9 Electrocatalytic efficiency of H_2 production over b-$NiMoO_4$ at a potential of ca. -0.3 V, measured for 60 min.

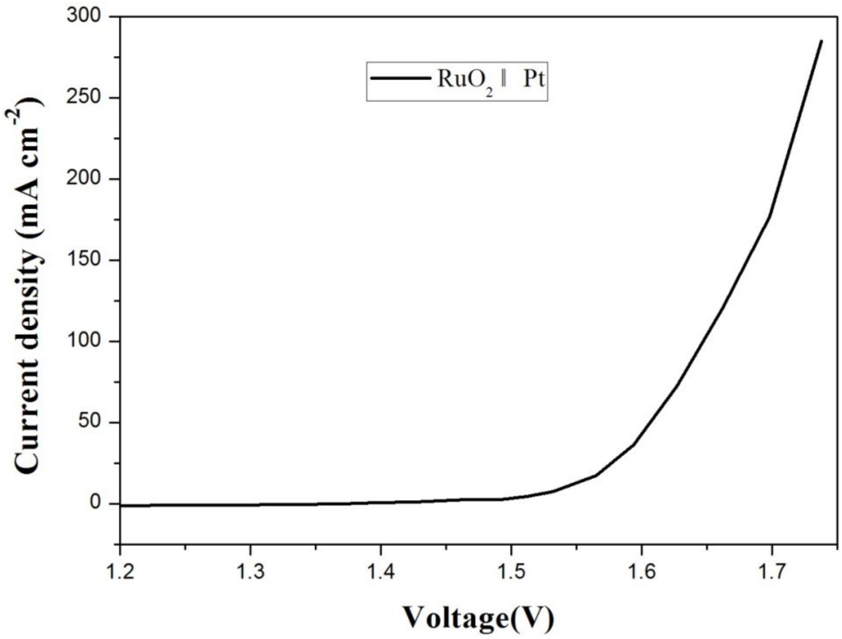

Fig. S10 Polarization curve of the RuO_2 and Pt for water splitting with a scan rate of 5 mV s^{-1} in 1 M KOH.

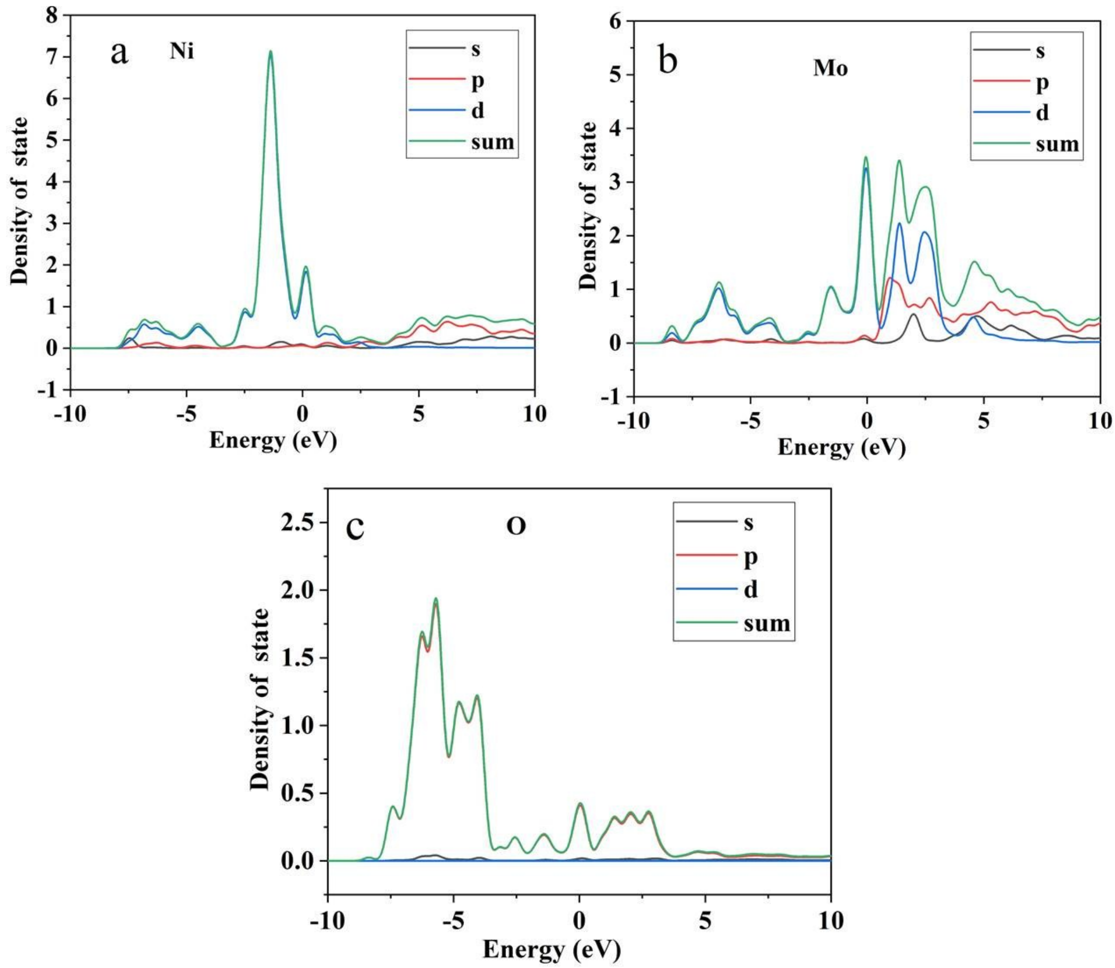

Fig. S11 Calculated density of states for Ni , Mo and O in a-$NiMoO_4$.

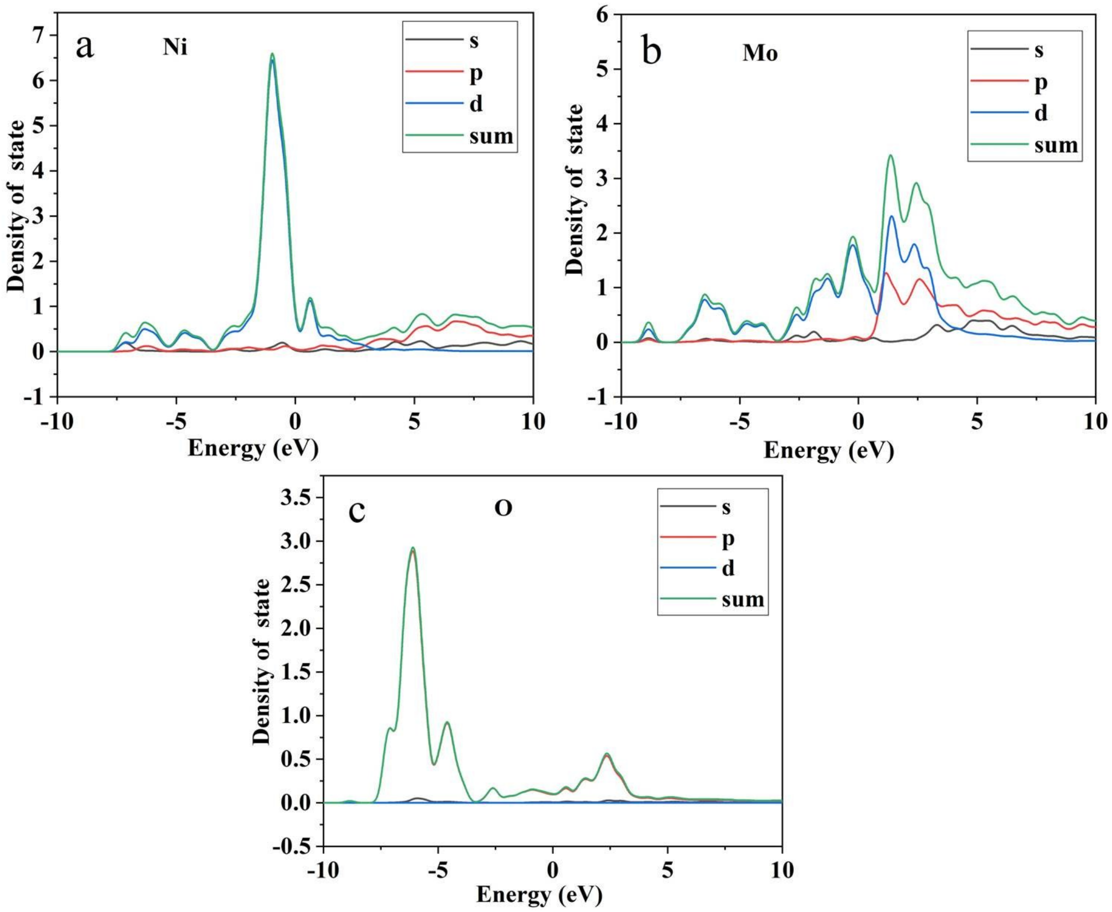

Fig. S12 Calculated density of states for Ni , Mo and O in b-$NiMoO_4$.

Res.

[1] S. Huang, Y. Meng, S. He, A. Goswami, Q. Wu, J. Li, S. Tong, T. Asefa, M. Wu, N-, O-, and S-Tridoped Carbon-Encapsulated Co9S8 Nanomaterials: Efficient Bifunctional Electrocatalysts for Overall Water Splitting, Adv.Funct. Mater. 27 (2017) 1606585.

[2] J. Duan, S. Chen, C. Zhao, Ultrathin metal-organic framework array for efficient electrocatalytic water splitting, Nat. Commun. 8 (2017) 15341.

[3] R. Zhang, C. Tang, R. Kong, G. Du, A.M. Asiri, L. Chen, X. Sun, Al-Doped CoP nanoarray: a durable water-splitting electrocatalyst with superhigh activity, Nanoscale 9 (2017) 4793-4800.

[4] H. Liu, X. Liu, Z. Mao, Z. Zhao, X. Peng, J. Luo, X. Sun, Plasma-activated Co3(PO4)2 nanosheet arrays with Co3+-Rich surfaces for overall water splitting, J.Power Sources 400 (2018) 190-197.

[5] X. Du, Z. Yang, Y. Li, Y. Gong, M. Zhao, Controlled synthesis of Ni(OH)2/Ni3S2 hybrid nanosheet arrays as highly active and stable electrocatalysts for water splitting, J. Mater. Chem. A 6 (2018) 6938-6946.

[6] Y. Gong, Z. Yang, Y. Zhi, Y. Lin, T. Zhou, J. Li, F. Jiao, W. Wang, Controlled synthesis of bifunctional particle-like Mo/Mn-NixSy/NF electrocatalyst for highly efficient overall water splitting, Dalton Trans. 48 (2019) 6718-6729.

[7] T. Zhu, L. Zhu, J. Wang, G.W. Ho, In situ chemical etching of tunable 3D Ni_3S_2 superstructures for bifunctional electrocatalysts for overall water splitting, J. Mater. Chem. A 4 (2016) 13916-13922.